Harla Journals

Harla Journal of Applied Science and Materials

Journal home page: https://journals.ddu.edu.et/index.php/HJASM

Harla journal of Applied Science and Materials

Temperature dependent upper critical magnetic field in $CePt_3Si$ superconductor

Habtamu Anagaw [1*], [2]Gebregziabher Kahsay and [2]Tamiru Negussie

[1]Department of physics, College of Natural and Computational Sciences, Dire Dawa University, Dire Dawa, Ethiopia

[2]Department of physics, College of Science, Bahir Dar University, Bahir Dar, Ethiopia

Abstract

The theoretical analysis of the temperature-dependent upper critical magnetic field is the main objective of this work. The temperature-dependent upper critical magnetic field (H_{C2}) in the superconductor $CePt_3Si$ is the main theoretical focus of this work. We demonstrate a clear correlation between the upper critical magnetic fields $H_{C2}^{||c}$(T), $H_{C2}^{\perp c}(T)$, $H_{C2}(\theta)$, the Ginzburg-Landau (GL) coherence length (ξ_{GL}), and the penetration depth (λ_{GL}) with temperature, using the GL phenomenological equation. We have plotted the phase diagram of H_{C2}, ξ_{GL}, and λ_{GL} versus temperature for $CePt_3Si$. Accordingly, the upper critical magnetic field decreases as temperature increases, eventually vanishing at the superconducting critical temperature of $CePt_3Si$. At the same time, the GL coherence length and GL penetration depth increase with temperature and approach infinity at the critical temperature, resulting in the breakdown of superconductivity. Our findings are consistent with previous experimental results.

Keywords: $CePt_3Si$, heavy fermion superconductor, upper critical magnetic field, GL coherence length, GL penetration depth.

1. Introduction

A material's ability to conduct electricity at low temperatures is known as superconductivity [1]. Every superconductor has a transition temperature (T_C) that causes it to return to its normal state above and show superconductivity below. The transition from a normal state to a superconducting state is shown by the lack of electrical resistance at low temperatures. It is thought that electricity can flow continuously for a long time without attenuation or decay in a closed superconducting circuit. The magnetic field is a key component in the field of superconductivity. Superconductors are categorized as type I or type II based on how they react to an applied magnetic field. An external magnetic field strong enough to damage a material's superconducting state can be applied [2].

**Corresponding author: Habtamu Anagaw; email: habtana@gmail.com ; Cell phone: +251913794716*

Received: September 2024; Received in revised form: October 2024; Accepted: December 2024

As an alternative to strong electron-electron interactions, heavy fermion compounds offer spin fluctuations, as many of these systems are approaching magnetic instability or show weak magnetic order. By adjusting control parameters like doping or pressure, these materials can be tuned around a quantum critical point, where magnetic fluctuations are probably responsible for the formation of Cooper pairs and superconductivity frequently appears. Cooper pairs in these situations may adopt spin-singlet or spin-triplet configurations since they can arise in various angular momentum pathways. Lines or points may serve as nodes when the gap disappears, resulting in a highly anisotropic gap caused by the orbital angular momentum.

Furthermore, these Cooper pairs of heavy particles carry the supercurrent. While spin-triplet pairing necessitates an inversion center, spin-singlet Cooper pairing can happen with time-reversal symmetry. The difference between odd-parity (spin-triplet) and even (spin-singlet) pairing is lost in systems without inversion symmetry, resulting in a mixing of spin channels. The upper critical magnetic field (H_{C2}) thus rises dramatically [3, 4 and 5].

Among the special kinds of superconductors are cerium-based heavy-fermion compounds. Mostly developed under hydrostatic pressure, they show superconductivity at a quantum critical point. Heavy fermion superconductors based on cerium include $CeCu_2Si_2(T_C = 0.6K)$ [6], $CeCoIn_5(T_C = 2.3K)$[7], $CeIrIn_5(T_C = 0.4K)$[8] , $CePt_3Si(T_C = 0.75K)$[9].

Cerium-based heavy-fermion compounds are a unique class of superconductors. Most of them exhibit superconductivity at a quantum critical point, typically achieved under hydrostatic pressure. Notable examples of cerium-based heavy-fermion superconductors include $CeCu_2Si_2(T_C = 0.6K)$ [6], $CeCoIn_5(T_C) = 2.3K$[7], $CeIrIn_5(T_C = 0.4K)$ [8], $CePt_3Si(T_C = 0.75K)$ [9].

The unusual crystal structure of the heavy-fermion superconductor $CePt_3$ Si is due to its lack of a center of symmetry, or inversion symmetry (non-centrosymmetric), which means that there isn't a mirror plane along the c-axis. It has garnered a lot of attention from academics because its lack of an inversion center alters its physical characteristics, resulting in antisymmetric spin-orbit coupling [3, 10].

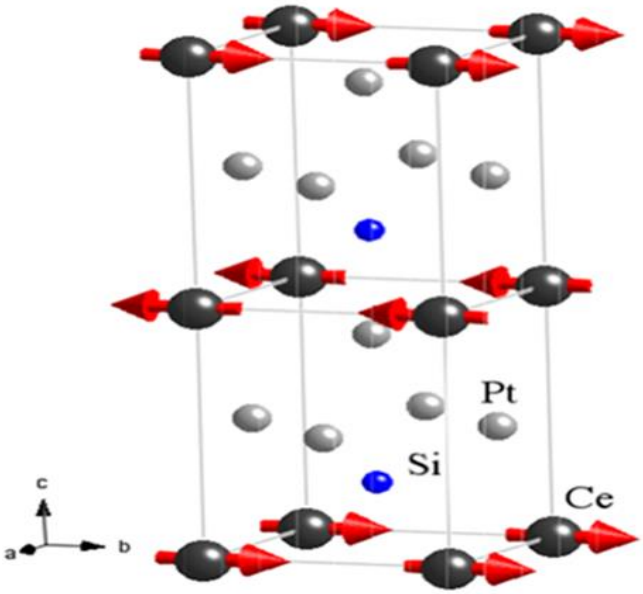

Figure 1. Crystal and magnetic structure of $CePt_3Si$. a) The arrows on the C_e - atoms indicate the magnetic moment lying in the basal c – plane [10].

$CePt_3Si$ crystallizes in a tetragonal structure with the space group P4mm and lattice parameters a = 0.4072 nm and c = 0.5442 nm [11–12]. The upper critical fields are $H_{C2}^{||a}(0)$ = 3.2 T and $H_{C2}^{||a}(0) = H_{C2}^{||ab}(0) = 2.7T$ [13]. This compound exhibits antiferromagnetic (AFM) order with a Néel temperature of T_N = 2.2 K and enters a heavy-fermion superconducting state below T_C = 0.75 K. In $CePt_3Si$, the upper critical field $H_{C2}(0)$ = 5 T exceeds the paramagnetic limiting field, intensely suggesting the existence of pure spin-triplet pairing [13].

2. Mathematical Formulations

2.1 Upper critical Magnetic field

By reducing the multi-band $CePt_3Si$ superconductor to a two-band model and employing wave functions for the superconducting order parameters Ψ_1 and Ψ_2, the upper critical magnetic field in the Ginzburg-Landau (GL) free energy density functional is theoretically investigated as follows [14–18].

$$F_{SC} = f_1 + f_2 + f_{12} + \frac{H^2}{8\pi} \quad (1)$$

$$f_1 = \left(-\frac{\hbar^2}{2m_1^*}\right)\left|\left(\nabla - \frac{2ieA}{\hbar c}\right)\Psi_1\right|^2 - \alpha_1|\Psi_1|^2 + \frac{\tau_1}{2}|\Psi_1|^4 \quad (2)$$

$$f_2 = \left(-\frac{\hbar^2}{2m_2^*}\right)\left|\left(\nabla - \frac{2ieA}{\hbar c}\right)\Psi_1\right|^2 - \alpha_2|\Psi_2|^2 + \frac{\tau_2}{2}|\Psi_2|^4 \quad (3)$$

$$f_{12} = \sigma(\Psi_1\Psi_2^* + \Psi_2\Psi_1^*) + \sigma_1\begin{pmatrix}\left[\left(\nabla + \frac{2ieA}{\hbar c}\right)^*\Psi_1^*\left(\nabla - \frac{2ieA}{\hbar c}\right)\Psi_2\right] \\ + \left[\left(\nabla + \frac{2ieA}{\hbar c}\right)^*\Psi_2^*\left(\nabla - \frac{2ieA}{\hbar c}\right)\Psi_1\right]\end{pmatrix} \quad (4)$$

where f_1 and f_2 are the free energies for each band, f_{12} the interaction free energy term of inter-band coupling of order parameters, $\frac{H^2}{8\pi}$ the energy stored in the local magnetic fields. The inter-band mixing of the gradients of the two order parameters and the inter-band interaction between the two order parameters are represented by the coefficients σ and σ_1. The effective masses of the charge carriers for the two bands are m_1^* and m_2^*. The temperature-dependent Ginzburg-Landau parameter is α, whereas the temperature-independent ones are τ_1 and τ_2. The vector potential is denoted by A.

Inserting Eqs. (2-4) into Eq. (1), we obtain,

$$F_{SC} = -\frac{\hbar^2}{2m_1^*}\left|\left(\nabla - \frac{2ieA}{\hbar c}\right)\Psi_1\right|^2 - \alpha_1|\Psi_1|^2 + \frac{\tau_1}{2}|\Psi_1|^4 - \frac{\hbar^2}{2m_2^*}\left|\left(\nabla - \frac{2ieA}{\hbar c}\right)\Psi_2\right|^2 - \alpha_2|\Psi_2|^2 + \frac{\tau_2}{2}|\Psi_2|^4 + \sigma(\Psi_1\Psi_2^* + \Psi_2\Psi_1^*) + \sigma_1\left(\left[\left(\nabla + \frac{2ieA}{\hbar c}\right)^*\Psi_1^*\left(\nabla - \frac{2ieA}{\hbar c}\right)\Psi_2\right] + \left[\left(\nabla + \frac{2ieA}{\hbar c}\right)^*\Psi_2^*\left(\nabla - \frac{2ieA}{\hbar c}\right)\Psi_1\right]\right) + \frac{H^2}{8\pi} \quad (5)$$

We reduce Eq. (5) in the following way to obtain the Ginzburg-Landau equation for two-band model superconductors.

$$\frac{\partial F_{SC}}{\partial \Psi_1^*} = 0 \quad (6a)$$

$$\frac{\partial F_{SC}}{\partial \Psi_2^*} = 0 \quad (6b)$$

As $\rightarrow T_C$, the higher-order terms are neglected. Eqs. (6.1) and (6.2), the reduced Ginzburg-Landau free energy density function becomes:

$$-\frac{\hbar^2}{2m_1^*}\left(\nabla - \frac{2ieA}{\hbar c}\right)^2\Psi_1 - \alpha_1\Psi_1 + \sigma\Psi_2 + \sigma_1\left(\nabla - \frac{2ieA}{\hbar c}\right)^2\Psi_2 = 0 \quad (7a)$$

$$-\frac{\hbar^2}{2m_1^*}\left(\nabla-\frac{2ieA}{\hbar c}\right)^2\Psi_2-\alpha_2\Psi_2+\sigma\Psi_1+\sigma_1\left(\nabla-\frac{2ieA}{\hbar c}\right)^2\Psi_1=0$$

(7 b)

Now, employing matrix notation, Eq. (7) can be written as,

$$\begin{bmatrix}f_{11} & f_{12}\\ f_{21} & f_{22}\end{bmatrix}\begin{pmatrix}\Psi_1\\ \Psi_2\end{pmatrix}=\begin{bmatrix}-\frac{\hbar^2}{2m_1^*}\left(\nabla-\frac{2ieA}{\hbar c}\right)^2-\alpha_1 & \sigma+\sigma_1\left(\nabla-\frac{2ieA}{\hbar c}\right)^2\\ \sigma+\sigma_1\left(\nabla-\frac{2ieA}{\hbar c}\right)^2 & -\frac{\hbar^2}{2m_2^*}\left(\nabla-\frac{2ieA}{\hbar c}\right)^2-\alpha_2\end{bmatrix}\begin{pmatrix}\Psi_1\\ \Psi_2\end{pmatrix}=0$$

(8)

Now, we can linearize Eq. (8) for the applied external magnetic field parallel to the c-axis and obtain:

$$f_{11}\Psi_1=-\frac{\hbar^2}{2m_1^*}\left(\nabla-\frac{2ieA}{\hbar c}\right)^2\Psi_1=\in_{11}\Psi_1$$

(9)

$$f_{22}\Psi_2=-\frac{\hbar^2}{2m_2^*}\left(\nabla-\frac{2ieA}{\hbar c}\right)^2\Psi_2=\in_{22}\Psi_2$$

(10)

Thus, Eqs. (9) and (10) become,

$$\begin{bmatrix}\in_{11}-\alpha_1 & \sigma+\sigma_1\left(\nabla-\frac{2ieA}{\hbar c}\right)^2\\ \sigma+\sigma_1\left(\nabla-\frac{2ieA}{\hbar c}\right)^2 & \in_{22}-\alpha_2\end{bmatrix}\begin{pmatrix}\Psi_1\\ \Psi_2\end{pmatrix}=0$$

(11)

The upper critical magnetic field can be calculated by considering the energy eigenvalues of the quantum harmonic oscillator. With the lowest energy levels $\in_{11}=\frac{1}{2}\hbar\omega_1$ and $\in_{22}=\frac{1}{2}\hbar\omega_2$, the upper critical magnetic field at the ground state can be represented as a harmonic oscillation with frequency $\omega_i=\frac{2eH_{C2}}{m_ic}$ and vector potential $\boldsymbol{A}=H_{C2}X$ in one dimension. Thus, Eq. (11) becomes:

By taking into account the energy eigenvalues of the quantum harmonic oscillator, the upper critical magnetic field may be computed. The upper critical magnetic field at the ground state can be described as a harmonic oscillation with frequency $\omega_i=\frac{2eH_{C2}}{m_ic}$ and vector potential $A=H_{C2}X$ in one dimension with the lowest energy levels $\in_{11}=\frac{1}{2}\hbar\omega_1$ and $\in_{22}=\frac{1}{2}\hbar\omega_2$. Eq. (11) thus becomes:

$$\begin{bmatrix}\frac{\hbar eH_{C2}}{m_1^*c}-\alpha_1 & \sigma-\sigma_1\frac{2eH_{C2}}{\hbar c}\\ \sigma-\sigma_1\frac{2eH_{C2}}{\hbar c} & \frac{\hbar eH_{C2}}{m_2^*c}-\alpha_2\end{bmatrix}\begin{pmatrix}\Psi_1\\ \Psi_2\end{pmatrix}=0$$

(12)

Assume $m_1^*=m_2^*=m^*$. Eq. (12) becomes,

$$\begin{vmatrix}\frac{\hbar eH_{C2}}{m^*c}-\alpha_1 & \sigma-\sigma_1\frac{2eH_{C2}}{\hbar c}\\ \sigma-\sigma_1\frac{2eH_{C2}}{\hbar c} & \frac{\hbar eH_{c2}}{m^*c}-\alpha_2\end{vmatrix}=0$$

(13)

Taking the determinant of the matrix of Eq. (13) and making some rearrangements gives,

$$\left[\left(\frac{e\hbar}{m^*c}\right)^2-\frac{4e^2\sigma_1^2}{\hbar^2c^2}\right]H_{C2}^2-\left[\frac{e\hbar}{m^*c}(\alpha_1+\alpha_2)-\frac{4e\sigma\sigma_1}{\hbar c}\right]H_{C2}+\alpha_1\alpha_{2-\sigma^2}=0 \quad (14)$$

This is a quadratic equation that can be solved using the quadratic formula, yielding:

$$H_{C2}=\frac{\frac{e\hbar}{m^*c}(\alpha_1+\alpha_2)-\frac{4e\sigma\sigma_1}{\hbar c}}{2\left[\left(\frac{e\hbar}{m^*c}\right)^2-\frac{4e^2\sigma_1^2}{(\hbar c)^2}\right]}\pm\frac{\sqrt{\frac{(e\hbar)^2[\alpha_1^2+\alpha_2^2]}{(m^*c)^2}-\frac{2(e\hbar)^2}{(m^*c)^2}\alpha_1\alpha_2-\frac{8e^2\sigma\sigma_1}{m^*c^2}[\alpha_1+\alpha_2]+\frac{16e^2\sigma_1^2}{(\hbar c)^2}\alpha_1\alpha_2+\frac{4\hbar^2\sigma^2}{(m^*c)^2}}}{2\left[\left(\frac{e\hbar}{m^*c}\right)^2-\frac{4e^2\sigma_1^2}{(\hbar c)^2}\right]} \quad (15)$$

Now, let $\alpha_1=\frac{\hbar^2}{2m^*\xi_{GL1}^2}$, $\alpha_2=\frac{\hbar^2}{2m^*\xi_{GL2}^2}$ and $\sigma=\frac{\hbar^2}{2m^*\xi_{GL12}^2}$; where $\xi_{GL1}^2,\xi_{GL2}^2,and\ \xi_{GL12}^2$ are the corresponding effective coherence lengths for each band. $\sigma_1=\frac{\eta\hbar^2}{2m^*}$ is the excitation energy, with η representing the gradient of inter-band mixing of the two order parameters in energy units, and $\Phi_0=\frac{2\pi\hbar}{e}$ is the magnetic flux quantization. Hence, the expression for H_{C2} becomes:

$$H_{C2}=\frac{\Phi_0}{2\pi(1-\eta^2)}\left(\frac{1}{2\xi_{GL1}^2}-\frac{1}{2\xi_{GL2}^2}+\frac{1}{2\xi_{GL12}^2}\right)\pm\frac{\Phi_0}{2\pi(1-\eta^2)}.\left[\left(\frac{1}{2\xi_{GL1}^2}-\frac{1}{2\xi_{GL2}^2}+\frac{1}{2\xi_{GL12}^2}\right)^2-(1-\eta^2)\left(\frac{1}{\xi_{GL1}^2\xi_{GL2}^2}-\frac{1}{\xi_{GL12}^4}\right)\right]^{\frac{1}{2}} \quad (16)$$

To solve Eq. (16), let us consider the following cases.

Case I: If $\left(\frac{1}{2\xi_{GL1}^2}-\frac{1}{2\xi_{GL2}^2}+\frac{1}{2\xi_{GL12}^2}\right)^2<<(1-\eta^2)\left(\frac{1}{\xi_{GL1}^2\xi_{GL2}^2}-\frac{1}{\xi_{GL12}^4}\right)$

In this case, the solution yields a complex result and will be ignored.

Case II: If $\left(\frac{1}{2\xi_{GL1}^2}-\frac{1}{2\xi_{GL2}^2}+\frac{1}{2\xi_{GL12}^2}\right)^2>>(1-\eta^2)\left(\frac{1}{\xi_{GL1}^2\xi_{GL2}^2}-\frac{1}{\xi_{GL12}^4}\right)$

Now, using the Taylor series expansion, the upper-critical magnetic field becomes,

$$H_{C2}=\frac{\Phi_0}{2\pi(1-\eta^2)}\left(\frac{1}{2\xi_{GL1}^2}+\frac{1}{2\xi_{GL2}^2}-\frac{\eta}{\xi_{GL12}^2}\right)-\frac{\Phi_0}{4\pi}\frac{\left(\frac{1}{\xi_{GL1}^2\xi_{GL2}^2}-\frac{1}{\xi_{GL12}^4}\right)}{\left(\frac{1}{2\xi_{GL1}^2}+\frac{1}{2\xi_{GL2}^2}-\frac{\eta}{\xi_{GL12}^2}\right)}+\frac{\Phi_0}{16\pi}\left(\frac{(1-\eta^2)\left(\frac{1}{\xi_{GL1}^2\xi_{GL2}^2}-\frac{1}{\xi_{GL12}^4}\right)^2}{\left(\frac{1}{2\xi_{GL1}^2}+\frac{1}{2\xi_{GL2}^2}-\frac{\eta}{\xi_{GL12}^2}\right)^3}\right) \quad (17)$$

Due to the drag effect [19], the two-band superconductor in Ginzburg-Landau (GL) theory is reduced to an effective single-band superconductor, such that $\alpha_2=\sigma=\sigma_1$. As a result, only the upper critical magnetic field is considered, and the simplified theory yields a solution to Eq. (19) for an effective single-band model.

Thus we get,

Considering the impact of the anisotropic mass tensor in Eq. (18), the Ginzburg-Landau coherence length will be incorporated into the expression for the upper critical magnetic field, yielding:

$$H_{C2} = \frac{\Phi_0}{2\pi\xi^2_{GL12}\sqrt{sin^2\theta+\gamma^2cos^2\theta}}\left(\frac{\xi^2_{GL12}}{\xi^2_{GL1}}+\frac{\xi^2_{GL12}}{\xi^2_{GL2}}-2\eta\right)\left[\frac{1}{1-\eta^2}-\frac{\frac{\xi^2_{GL12}}{\xi^2_{GL1}\xi^2_{GL2}}-1}{\left(\frac{\xi^2_{GL12}}{\xi^2_{GL1}}+\frac{\xi^2_{GL12}}{\xi^2_{GL2}}-2\eta\right)^2}+\frac{(1-\eta^2)\left(\frac{\xi^4_{GL12}}{\xi^2_{GL1}\xi^2_{GL2}}-1\right)^2}{\left(\frac{\xi^2_{GL12}}{\xi^2_{GL1}}+\frac{\xi^2_{GL12}}{\xi^2_{GL2}}-2\eta\right)^4}\right] \quad (19)$$

The effective GL coherence length (ξ^2_{GLeff}) is expressed as,

$$\frac{1}{\xi^2_{GLeff}} = \frac{1}{\xi^2_{GL12}}\left(\frac{\xi^2_{GL12}}{\xi^2_{GL1}}+\frac{\xi^2_{GL12}}{\xi^2_{GL2}}-2\eta\right)\left[\frac{1}{1-\eta^2}-\frac{\frac{\xi^2_{GL12}}{\xi^2_{GL1}\xi^2_{GL2}}-1}{\left(\frac{\xi^2_{GL12}}{\xi^2_{GL1}}+\frac{\xi^2_{GL12}}{\xi^2_{GL2}}-2\eta\right)^2}+\frac{(1-\eta^2)\left(\frac{\xi^4_{GL12}}{\xi^2_{GL1}\xi^2_{GL2}}-1\right)^2}{\left(\frac{\xi^2_{GL12}}{\xi^2_{GL1}}+\frac{\xi^2_{GL12}}{\xi^2_{GL2}}-2\eta\right)^4}\right] \quad (20)$$

Then, Eq. (19) becomes,

$$H_{C2}(T) = \frac{\Phi_0}{2\pi\xi^2_{GLeff}(T)\sqrt{sin^2\theta+\gamma^{-2}cos^2\theta}} \quad (21)$$

From Eq. (18), the expression for the upper critical magnetic field $H^{||c}_{C2}$ when the applied magnetic field is parallel to the c-axis becomes:

$$H^{||c}_{C2}(T) = H^{||c}_{C2}(0)\left[1-\left(\frac{T}{T_c}\right)\right] \quad (22)$$

where, $H^{||c}_{C2}(0) = \frac{\Phi_0}{2\pi(\xi^{ab}_{GL})^2(0)}$ is the zero temperature upper critical magnetic field parallel to the c- axis.

If the direction of the applied magnetic field is perpendicular to the c-axis, then the expression for the upper critical magnetic field $H^{\perp c}_{C2}(T)$ in Eq. (18) becomes,

$$H^{\perp c}_{C2}(T) = H^{\perp c}_{C2}(0)\left[1-\left(\frac{T}{T_c}\right)\right] \quad (23)$$

where, $H^{\perp c}_{C2}(0) = \frac{\Phi_0}{2\pi\xi^{ab}_{GL}(0)\xi^{c}_{GL}(0)}$ is the zero temperature upper critical magnetic field perpendicular to the c- axis.

Now, using Eq. (21), we can determine the angle dependence of the upper critical magnetic field for isotropic effective masses at an angle between the c-axis and the applied magnetic field at low temperatures. That is:

$$H^{GL}_{C2}(\theta) = \frac{\Phi_0}{2\pi\xi^2_{GLeff}(0)\sqrt{sin^2\theta+\gamma^{-2}cos^2\theta}} \quad (24)$$

From the experimental values, we have $H^{||ab}_{C2}(0) = 2.7$ T, $H^{||c}_{C2}(0) = 3.2$ T, $H^{||a}_{C2}(0) = H^{\perp c}_{C2}(0) = 2.7$ T [20] and $\Phi_0 = 2.068\times10^{-15}\,Wb$. Thus, using Eqs. (22) and (23), along with $T_C = 0.75$ K, the mathematical expressions for the temperature dependence of the upper critical magnetic field, both parallel and perpendicular to the symmetry axes in $CePt_3Si$ are expressed as,

$$H^{||c}_{C2}(T) = 3.2\text{Tesla}\left[1-\left(\frac{T}{T_C}\right)\right] \quad (25)$$

$$\mathrm{H}_{\mathrm{C2}}^{||ab}(\mathrm{T}) = \mathrm{H}_{\mathrm{C2}}^{\perp c}(\mathrm{T}) = 2.7\ \mathrm{Tesla}\left[1-\left(\frac{T}{C}\right)\right] \quad (26)$$

The upper critical magnetic field anisotropy deduced from measurements parallel and perpendicular to the c-axis is small, i.e. $\frac{\mathrm{H}_{\mathrm{C2}}^{||c}(0)}{\mathrm{H}_{\mathrm{C2}}^{\perp c}(0)} \approx 1.2$ for $\mathrm{T} \to 0$.

The pressure dependence of the upper critical magnetic field is found to be:

$$\mathrm{H}_{\mathrm{C2}}^{||a}(\mathrm{T}) = \mathrm{H}_{\mathrm{C2n}}(0)(\mathrm{P})\left[1-\left(\frac{T}{T_{Cn}}\right)\right] \quad (27)$$

where, $\mathrm{H}_{\mathrm{C2n}}$ and T_{Cn} are the upper critical magnetic field and the critical temperature values at each pressure respectively.

Using experimental values for $H_{C2n}(0)$ at T_{Cn} at different pressure values, with $\mathrm{H}_{\mathrm{C2}}(0) = 2.7\ \mathrm{T}$ at $P_1 = 0$, $\mathrm{H}_{\mathrm{C2}}(0) = 1.8\mathrm{T}$ at $P_2 = 0.1\mathrm{GPa}$, $\mathrm{H}_{\mathrm{C2}}(0) = 0.9\mathrm{T}$ at $P_3 = 0.4\mathrm{GPa}$, $\mathrm{H}_{\mathrm{C2}}(0) = 0.6\mathrm{T}$ at $P_4 = 0.6\mathrm{GPa}$ and $\mathrm{H}_{\mathrm{C2}}(0) = 0.1\mathrm{T}$ at $P_5 = 1.2\mathrm{GPa}$ with 0.75K, 0.7K, 0.43K, 0.33K and 0.18K [21] becomes,

$$\mathrm{H}_{\mathrm{C2}}^{||a}(\mathrm{T}) = 2.7\left[1-\left(\frac{T}{T_{C1}}\right)\right] \quad (27a)$$

$$\mathrm{H}_{\mathrm{C2}}^{||a}(\mathrm{T}) = 1.85\left[1-\left(\frac{T}{T_{C2}}\right)\right] \quad (27b)$$

$$\mathrm{H}_{\mathrm{C2}}^{||a}(\mathrm{T}) = 0.9\left[1-\left(\frac{T}{T_{C3}}\right)\right] \quad (27c)$$

$$\mathrm{H}_{\mathrm{C2}}^{||a}(\mathrm{T}) = 0.65\left[1-\left(\frac{T}{T_{C4}}\right)\right] \quad (27d)$$

$$\mathrm{H}_{\mathrm{C2}}^{||a}(\mathrm{T}) = 0.1\left[1-\left(\frac{T}{T_{C5}}\right)\right] \quad (27e)$$

The effect of an anisotropic effective mass m^* on the angular dependence can be determined by using the GL theory as follows,

$$\left(\frac{H_{C2}^{GL}(\theta)\,sin\theta}{\mathrm{H}_{\mathrm{C2}}^{\perp c}}\right)^2 + \left(\frac{H_{C2}^{GL}(\theta)\,cos\theta}{\mathrm{H}_{\mathrm{C2}}^{||c}}\right)^2 = 1 \quad (28)$$

Finally, the angular dependence of the upper critical magnetic field for $CePt_3Si$ at an angle θ from the c-axis can be expressed as:

$$H_{C2}^{GL}(\theta) = \frac{\mathrm{H}_{\mathrm{C2}}^{||c}}{\sqrt{\gamma^2 sin^2\theta + cos^2\theta}} = \frac{3.2}{\sqrt{1.4\,sin^2\theta + cos^2\theta}},\ \gamma^2 = 1.4 \quad (29a)$$

$$H_{C2}^{GL}(\theta) = \frac{\mathrm{H}_{\mathrm{C2}}^{ab}}{\sqrt{\gamma^2 sin^2\theta + \gamma^2 cos^2\theta}} \quad (29b)$$

or

$$\frac{H_{C2}^{GL}(\theta)}{\mathrm{H}_{\mathrm{C2}}^{||c}(\mathrm{T})} = \frac{1}{3.2\mathrm{T}\left[1-\left(\frac{T}{T_c}\right)\right]\sqrt{sin^2\theta + \gamma^{-2}cos^2\theta}} \quad (29c)$$

where θ is the angle between the applied field and the c-axis.

2.2. Derivation of the of Ginzburg-Landau parameters

The distance over which superconductivity can change without experiencing excessive energy is defined by the GL coherence length $\xi_{GL}(T)$, which is the length scale over which the order

parameter ψ may fluctuate [22]. Using the GL model, we can derive expressions for superconducting parameters such as the GL coherence length (ξ_{GL}) , approximately equal to the vortex core radius) and the penetration depth ((λ_{GL}) as follows:

$$\xi_{GL}(T) = \left(\frac{\hbar^2}{2m^*|\alpha(T)|}\right)^{\frac{1}{2}} \quad (30)$$

But the GL temperature-dependent parameter $\alpha_i(T)$ is expressed as, $\alpha_i(T) = \alpha_0\left[1 - \left(\frac{T}{T_c}\right)\right]$ [23]. Thus, we obtain,

$$\xi_{GL}(T) = \xi_{GL}(0)\left[1 - \left(\frac{T}{T_c}\right)\right]^{-1/2} \quad (31)$$

where $\xi_{GL}(0)$, is the zero temperature coherence length.

Now, using $\xi^{||a}(0)$=11nm [24], $\xi_{GL}^{||c}(0)$=10nm, $\xi_{GL}^{||ab}(0) = 8.2nm$ and $\xi_{GL}^{||c}(0) = 9\,nm$ [25] in Eq. (33), we get,

$$\xi_{GL}^{||a}(T) = 11\text{nm}\left[1 - \left(\frac{T}{T_c}\right)\right]^{-1/2} \quad (32)$$

$$\xi_{GL}^{||ab}(T) = 8.2\text{nm}\left[1 - \left(\frac{T}{T_c}\right)\right]^{-1/2} \quad (33)$$

$$\xi_{GL}^{||c}(T) = 9.0\text{nm}\left[1 - \left(\frac{T}{T_c}\right)\right]^{-1/2} \quad (34)$$

The length scale associated with the Meissner effect is the Ginzburg-Landau (GL) penetration depth (λ_{GL}), which describes the depth of penetration of an externally applied magnetic field. Consequently, the term "magnetic screening length" is frequently used [22]. According to the Meissner effect, an external magnetic field is completely expelled from the interior of a superconductor. However, there is a growing capacity for magnetic fields to penetrate a superconductor and flow within a very thin layer. The thickness of this layer, known as the GL penetration depth, can be calculated using the superconducting electron density and is expressed as follows [24]:

$$\lambda_{GL}(T) = \left(\frac{m^*c^2}{16\pi e^2 n_s}\right)^{\frac{1}{2}} \quad (35)$$

If T→ 0, then $n_s \to n$.

where n and n_s are the total electron density and the superconducting electron density, respectively.

Thus we get,

$$\lambda_{GL}(0) = \left(\frac{m^*c^2}{16\pi e^2 n}\right)^{\frac{1}{2}} \quad (36)$$

Taking the ratio of Eq. (35) to Eq (36) gives:

$$\frac{\lambda_{GL}(T)}{\lambda_{GL}(0)} = \left(\frac{n}{n_s}\right)^{\frac{1}{2}} \text{ Or } \left(\frac{\lambda_{GL}(T)}{\lambda_{GL}(0)}\right)^{-2} = \left(\frac{n_s}{n}\right) \quad (37)$$

From the two-fluid model [26], we have:

$$\frac{n_s}{n} = \left[1 - \left(\frac{T}{T_C}\right)^4\right] \quad (38)$$

Combining Eqs. (37) and (38) to solve for $\lambda_{GL}(T)$, we get,

$$\lambda_{GL}(T) = \lambda_{GL}(0)\left[1 - \left(\frac{T}{T_c}\right)^4\right]^{-1/2} \quad (39)$$

Now employing, $H_{C2}(0) = 5$ T and $\mu_0 H_C(0) = 26$mT , we can obtain the value for the GL characteristic parameter($\kappa_{GL}) = \frac{H_{C2}(0)}{\sqrt{2}H_C} = 140$, which, in turn, determines $\lambda_{GL}(0)$. That is, $\lambda_{GL}(\mathrm{T} \to 0) = 1.11^{-6}$m [27].

$$\lambda_{GL}(T) = 1.11\mu\mathrm{m}\left[1 - \left(\frac{T}{T_C}\right)^4\right]^{-1/2} \quad (40)$$

3. Results and discussion

In this research, we have established the mathematical expressions and relationships between temperature, the upper critical magnetic field, and the Ginzburg-Landau (GL) characteristic lengths by using the well-known GL equation. Furthermore, the phase diagrams showing the effect of pressure on the upper critical magnetic field and the critical temperature of the two-band high-temperature superconductor $CePt_3Si$ have been plotted by employing Eqs. (25) and (26) along with some plausible experimental values at zero temperature [20,21]. As shown in Fig-2, the upper critical magnetic field decreases as the temperature increases and ultimately goes to zero at the superconducting critical temperature of $CePt_3Si$ which is to mean that the magnetic field will be expelled out from the surface of the superconductor which is the Meissner effect .The plot shows that H_{C2} has no significant anisotropy ($\frac{H_{C2}^{||c}(0)}{H_{C2}^{\perp c}(0)} \approx 1.2$) [28].

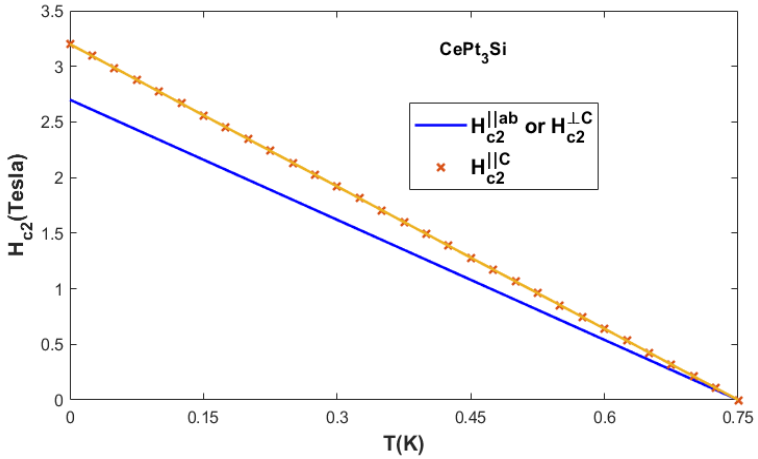

Figure 2. Upper critical magnetic field parallel to ab-plane and c -axis versus temperature for $CePt_3$ Si superconductor.

Now, using Eq. (27), we have plotted the phase diagram of the pressure-dependent upper critical field and superconducting critical temperature, as depicted in Fig-3. As observed from the figure, the superconducting critical temperature decreases with increasing pressure, from 0.75 K (at ambient pressure) to 0.19 K at 1.2 GPa. At the same time, the upper critical magnetic field

decreases from $H_{C2}(0) = 2.7\,T$(at ambient pressure) to $H_{C2}(0) = 0.1\,T$ (at 1.2 GPa) with the increase of applied external pressure along the a-axis. This is due to the antiferromagnetic and non-centrosymmetric nature of $CePt_3Si$, in which the applied pressure results in spin fluctuations, as superconductivity is correlated with the antiferromagnetic state and is concluded to be stable at ambient pressure. Our work is in good agreement with the experimental results [22].

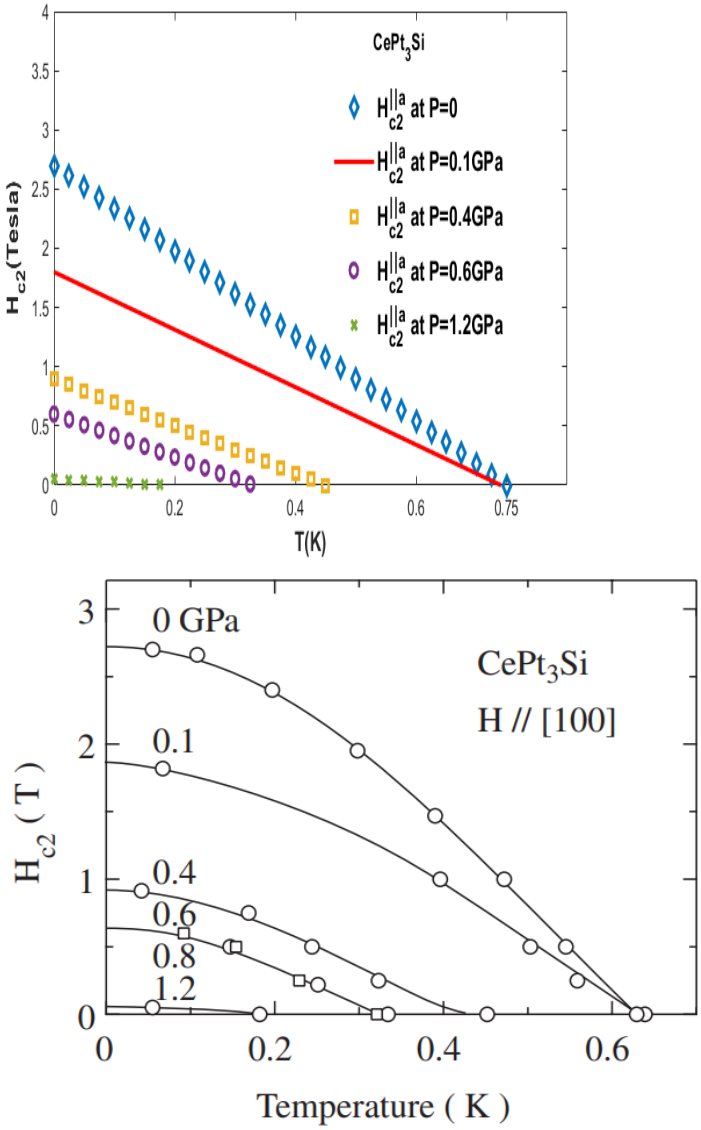

Figure 3. Pressure dependence of the upper critical magnetic field and critical temperature for $CePt_3Si$ superconductor(the left side(our work) and the right side (by Takashi Y. et al. (2004)).

Similarly, as shown in Fig. 4, the upper critical magnetic field slightly decreases as the angle increases from 0^0 to 90^0, reaching a value of $H_{C2}^{||a}$ =2.7T [22], indicating that the anisotropy of the angle-dependent upper critical field is very small. As $CePt_3Si$ is an antiferromagnetic superconductor, the spin arrangements are affected by changes in the direction of the applied field, which is why the upper critical magnetic field varies with changes in angle.

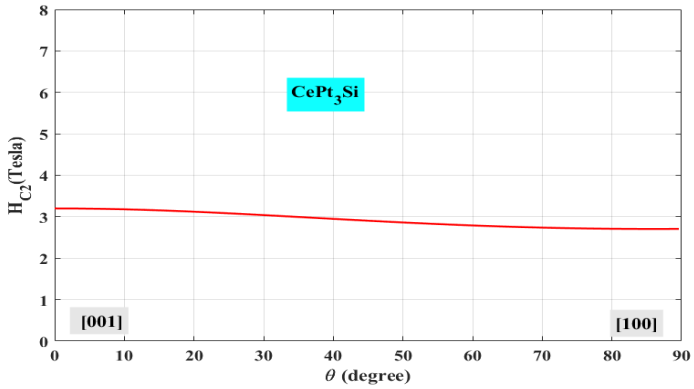

Figure 4. Angle dependence of upper critical magnetic field for $CePt_3Si$ superconductor.

Furthermore, using Eqs. (32-34) and some appropriate experimental values, the temperature dependence of the GL coherence lengths $\xi_{GL}^{ab}(T)$, $\xi_{GL}^{a}(T)$ and $\xi_{GL}^{c}(T)$ is plotted as depicted in Fig. 5. As observed from the figure, the GL coherence length increases slightly with rising temperature and approaches infinity at the superconducting critical temperature. This indicates that the breakdown of Cooper pairs occurs at the superconducting critical temperature of $CePt_3Si$, resulting in the vanishing of superconductivity.

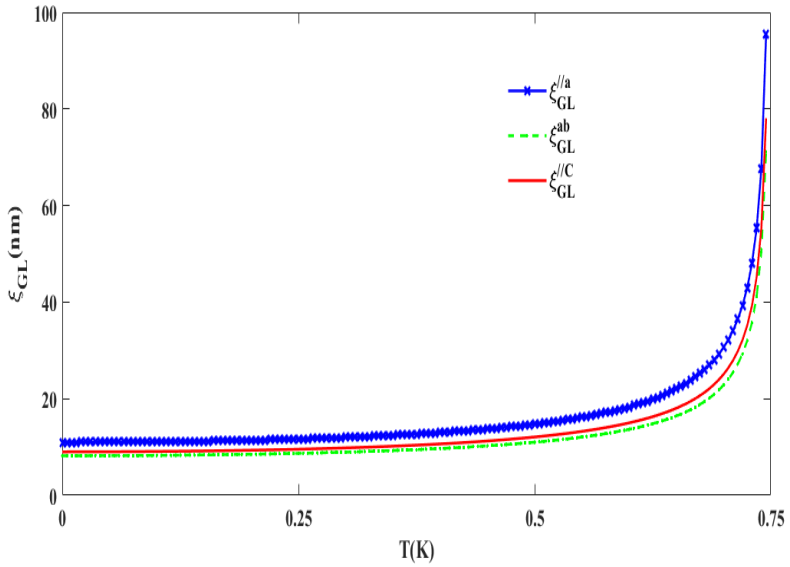

Figure 5. The temperature dependence of GL coherence length parallel to the three axes for $CePt_3Si$ superconductor.

Finally, the temperature dependence of the GL penetration depth has been plotted, as shown in Fig. 6. It can be observed from the figure that the penetration depth rises (diverges) asymptotically as the temperature approaches T_C. This indicates the suppression of superconductivity or the breakdown of Cooper pairs.

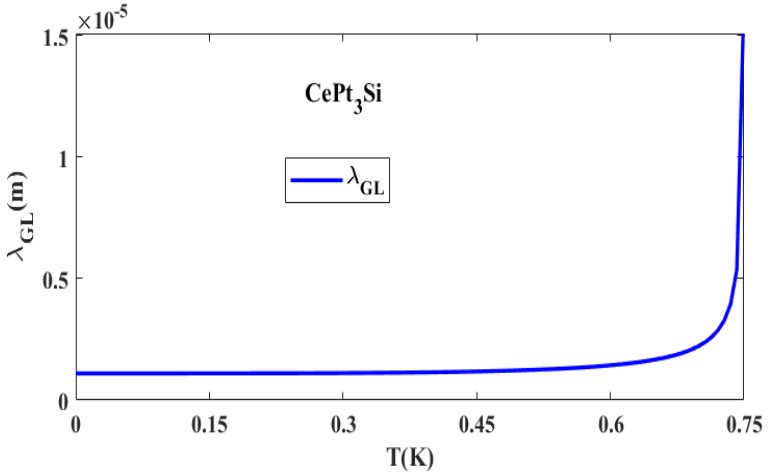

Figure 6. Temperature dependence of the GL penetration depth for $CePt_3Si$ superconductor.

4. Conclusion

In the current research, we have investigated the upper critical magnetic field, the GL coherence length, and the GL penetration depth for the multiband superconductor $CePt_3Si$ using the well-established GL phenomenological equation. We obtained the relationship between pressure, upper critical magnetic field, and superconducting critical temperature. Furthermore, phase diagrams were plotted using MATLAB software. From the plotted phase diagrams, we conclude that the upper critical magnetic field of the superconducting $CePt_3Si$ is inversely related to temperature, which is in agreement with previous findings [21, 22, 24–31]. Additionally, it can be observed from the phase diagrams that, as temperature rises, both the GL coherence length and the GL penetration depth increase asymptotically and diverge as $T \rightarrow T_c$, resulting in the disappearance of superconductivity. Moreover, pressure, the upper critical magnetic field, and the critical temperature for superconductivity are inversely related.

Using the well-known GL phenomenological equation, we have examined the upper critical magnetic field, the GL coherence length, and the GL penetration depth for the multiband superconductor $CePt_3Si$ in the present study. We were able to determine the correlation between superconducting critical temperature, pressure, and upper critical magnetic field. Additionally, MATLAB software was used to plot phase diagrams. We infer from the exhibited phase diagrams that the superconducting $CePt_3Si$'s upper critical magnetic field is inversely proportional to temperature, which is consistent with other results [21, 22, 24–31]. Furthermore, the phase diagrams show that superconductivity vanishes as temperature increases since the GL coherence length and the GL penetration depth both asymptotically increase and diverge as $T \rightarrow T_C$. Additionally, pressure, the

Acknowledgements

We acknowledge Bahir Dar University, Dire Dawa University and the Ministry of Education of Ethiopia for all support.

Conflict of interest

The authors declare that there is no conflict of interest.

References

1. Onnes, H.K.Akad.Weten Schappen(Amsterdam)**14**,113(1911).
2. Gennes, P. G. de, Superconductivity of Metals and Alloys, W. A. Benjamin, Inc., New York(1966).
3. E. Bauer, I. Bonalde, A. Eichler, et al. $CePt_3Si$: Heavy Fermion Superconductivity and Magnetic Order without Inversion Symmetry**,** AIP Conference Proceedings **850**, 695(2006): https://doi.org/10.1063/1.2354900.
4. Habtamu Anagaw, Gebregziabher Kahsay and Tamiru Negussie, Theoretical study of upper critical magnetic field in superconductor UTe_2, *Indian journal of physics* ***98***(2), *2273(2024)*: **https://doi.org/10.1007/s12648-023-03000-7**.
5. Habtamu Anagaw, Gebregziabher Kahsay and Tamiru Negussie, Thermodynamic and magnetic properties of superconductor UTe_2, *Physics of the Solid State* ***66****(9), (2024),* DOI: 10.1134/S1063783424600729
6. F. Steglich, J. Aarts, C.D. Bredl, W. Lieke, D. Meschede, W. Franz, Superconductivity in the Presence of Strong Pauli Paramagnetism: $CeCu_2Si_2$, Phys. Rev. **43**, (1979), DOI:10.1103/PhysRevLett.43.1892
7. T. Fukui, et al.,Surface Superconducting State of Heavy-Fermion Superconductor $CeIrIn_5$ Probed by $CeIrIn_5$ - Ag Junctions, Journal of Low Temperature Physics, **13**, (2003), https://doi.org/10.1023/A:1026083124132
8. H. Hegger, C. Petrovic, E.G. Moshopoulou, M.F. Hundley, J.L. Sarrao, Z. Fisk, J.D. Thompson, Pressure-Induced Superconductivity in Quasi-2D $CeRhIn_5$, Phys. Rev. **84**, (2000), DOI:10.1103/PhysRevLett.84.4986
9. N. Metoki, K. Kaneko, T.D. Matsuda, A. Galatanu, T. Takeuchi, S. Hashimoto, T. Ueda,R. Settai, Y.Onuki, N. Bernhoeft, Coexistence of Antiferromagnetism and Heavy-Fermion Superconductivity in $CePt_3Si$ Studied by Neutron Scattering, J. Phys. Soc. Jpn. **75**, 177(2006), https://journals.jps.jp/doi/10.1143/JPSJS.75S.177.
10. N. Metoki, K. Kaneko, T.D. Matsuda, A. Galatanu, T. Takeuchi, S. Hashimoto, T. Ueda, R. Settai, Y. Onuki, N.Bernhoeft, Magnetic structure and the crystal field excitation in heavy-fermion antiferromagnetic superconductor $CePt_3Si$, J. Phys.: Condens. Matter **16**, L333-L342 (2004), DOI: 10.1088/0953-8984/16/15/L01
11. A.I. Tursina, A.V. Gribanov, H. Noel, P. Rogl, Y.D. Seropegin, O.I. Bodak, Crystal structure of the new ternary silicide $CePt_3Si$, Journal of Alloys and Compounds **383**, 239(2004), https://doi.org/10.1016/j.jallcom.2004.04.069
12. E. Bauer, I. Bonalde, A. Eichler, G. Hilscher, Y. Kitaoka1, R. Lackner, St. Laumann, H. Michor, M. Nicklas, P. Rogl, E.W. Scheldt, M. Sigrist and M.Yogi, $CePt_3Si$:HeavyFermion Superconductivity and Magnetic Order without Inversion Symmetry, Applied Physics Letters **109**, 102601 (2016) ,https://doi.org/10.1063/1.2354900.
13. J. Chen1, L. Jiao1, J L Zhang, Y Chen, L Yang, M Nicklas, F Steglich and H Q Yuan,Heavy Evidence for two-gap superconductivity in the non-centrosymmetric compound $LaNiC_2$, New J. Phys. **15**, 053005(2013): DOI:10.1088/1367-2630/15/5/053005
14. L. A. Turkevich, Ginzburs-Landau theory of the upper critical field in filamentary superconductor, Phys. Rev. B, **19**, (1979), https://journals.aps.org/prb/pdf/10.1103/PhysRevB.19.2520.
15. I. N. Askerzade ,Anisotropy of the Upper Critical Field in MgB_2:The Two-Band Ginzburg–Landau Theory, JETP Letters, **81**, 583(2005) , DOI:10.1134/1.2029949.
16. Tsadik Kidanemariam and Gebregziabher Kahsay, Theoretical Study of Upper Critical Magnetic Field H_{C2} in Multiband Iron Based Superconductors, Advances in Condensed Matter Physics, **2016**(2), 2016, DOI:10.1155/2016/5470429.
17. P. Udomsamuthirun, A. Changjan, C. Kumvongsa and S.Yoksan, H_{C2} of anisotropy two-band superconductors by Ginzburg-Landau approach, Physica C, **434**, 6266(2006), DOI:10.1016/j.physc.2005.12.001.
18. J. Murphy, M. A. Tanatar, D. Graf, J. S. Brooks, S. L. Bud'ko, P. C. Canfield, V. G. Kogan, and R. Prozorov, Angular-dependent upper critical field of over doped $Ba(Fe_{(1-x)}\,Ni_x)_2As_2$, Phys. Rev. B, **87**, (2013) , DOI: 10.1103/PhysRevB.87.094505.
19. M. V. Boev, Photon drag of superconducting fluctuations in two-dimensional systems, Phys.Rev. B, **101**, 104512 (2020), DOI: 10.1103/PhysRevB.101.104512.
20. Christian Pfleiderer, Superconducting phases of f-electron compounds, Rev. of Mod. Phys., **81**, (2009), DOI: 10.1103/RevModPhys.81.1551.

21. E. Bauer, I. Bonalde, A. Eichler, et al., $CePt_3Si_3$: Heavy Fermion Superconductivity and Magnetic Order without Inversion Symmetry, AIP Conference Proceedings **850**, 695(2006), https://doi.org/10.1063/1.2354900.

22. Takashi Y Asuda et al., Superconducting Property in $CePt_3Si$ under Pressure, Journal of the Physical Society of Japan**73**,1657(2004), DOI:10.1143/JPSJ.73.1657.

23. P. Quarterman, Nathan Satchell, B. J. Kirby, Reza Loloee, Gavin Burnell , Norman O. Birge , and J. A. Borchers., Distortions to the penetration depth and coherence length of superconductor/normal-metal super lattices, Physical review materials **4**, 074801 (2020) , DOI: 10.1103/PhysRevMaterials.4.074801.

24. Gebregziabher Kahsay, Tamiru Negussie, Theoretical investigation of upper critical magnetic field (Hc_2) of the heavy fermion superconductor $CeRhIn_5$, Latin-American Journal of Physics Education ,**14** (3), 1 (2020), http://www.lajpe.org/sep20/14_3_04.pdf.

25. A.B. Pippard, The surface impedance of superconductors and normal metals at high frequencies (1950), https://royalsocietypublishing.org/doi/pdf/10.1098/rspa.1950.0134.

26. James F. Annett , Superconductivity, Superfluids and Condensates**(**2004).

27. E. Bauer, I. Bonalde and M. Sigrist ,Superconductivity and normal state properties of non centrosymmetric $CePt_3Si$, Low Temperature Physics **31**, 748 (2005), https://doi.org/10.1063/1.2008135.

28. E. Bauer , H. Kaldarar, A. Prokofiev, E. Royanian, A. Amato, J. Seren, W. Bramer-Escamilla and I. Bonalde, Heavy Fermion Superconductivity and Antiferromagnetic Ordering in $CePt_3Si$ without Inversion Symmetry, Journal of the Physical Society of Japan (2007), DOI: 10.1143/JPSJ.76.051009.

29. Rikio Settai, Tetsuya Takeuchi, and Yoshichika O nuki, Recent Advances in Ce-Based Heavy-Fermion Superconductivity and Fermi Surface Properties, Journal of the Physical Society of Japan **76**, 051003 (2007) , DOI: 10.1143/JPSJ.76.051003.

30. E. Bauer, G. Hilscher, H. Michor, Ch. Paul, E. W. Scheidt, A. Gribanov, Yu. Seropegin, H. Noël, M. Sigrist, and P. Rogl, Heavy Fermion Superconductivity and Magnetic Order in Noncentrosymmetric $CePt_3Si$, Phys. Rev. Lett. **92**, 027003 (2004), DOI: 10.1103/PhysRevLett.92.027003

31. Yoshichika Onuki, Yuuichiro Miyauchi1, Masahiko Tsujino, Yuki Ida, Rikio Settai, Tetsuya Takeuchi, Naoyuki Tateiwa, Tatsuma D. Matsuda, Yoshinori Haga and Hisatomo Harima, Superconducting Properties of $CePt_3Si$ and $CeIrSi_3$ without Inversion Symmetry in the Crystal Structure, J. Phys. Soc. Jpn. **77,** Suppl. A, pp. 37–42 (2008).